New Constraints on Gauge Mediation and Beyond from LHC SUSY Searches at 7 TeV

Matthew J. Dolan, David Grellscheid, Joerg Jaeckel, Valentin V. Khoze and Peter Richardson

Institute for Particle Physics Phenomenology, Department of Physics, Durham University, Durham DH1 3LE, United Kingdom

Abstract

The first results from the LHC on jets plus missing energy provide powerful new data to test SUSY models. Initial theoretical interpretations of these data have concentrated on gravity mediation, usually the CMSSM and its variations. In this paper we confront a large class of gauge mediation models with these new data. More precisely we consider models of pure general gauge mediation (pure GGM) and confront them with the recent experimental results of the ATLAS collaboration. We use Herwig++ and RIVET, incorporating the full set of experimental cuts, to calculate the signal rates and compare them to the data. Although based on only $35 \mathrm{pb}^{-1}$ of integrated luminosity, we show that these new data probe and exclude a portion of previously allowed parameter space of GGM.

In addition we investigate the viability of standard SUSY benchmark points, including the Snowmass, CMS and ATLAS sets which encompass other mediation scenarios such as gravity, anomaly and gaugino mediation.

1 Introduction

Recently the CMS and ATLAS collaborations conducted a first series of searches for supersymmetry in 7 TeV proton-proton collisions at the LHC looking for squarks and gluinos in final states containing jets and missing energy [1–4]. These analyses were based on 35 pb⁻¹ of data taken in 2010. As no excess above the Standard Model expectations was observed in these experiments, their results set limits on the sparticle production and consequentially provide stringent new constraints on the allowed regions of parameter spaces in SUSY models. So far, most of the theoretical analysis of these initial LHC searches has concentrated on constraining the CMSSM and related models [5–10] which are expected to arise from gravity mediation scenarios.

In this paper we will assess the impact of these searches for gauge mediated SUSY breaking models. The most stringent constraints on the CMSSM¹ currently come from the ATLAS zero-lepton searches [3]. Here we will concentrate upon these, and apply them to a concise class of General Gauge Mediation (GGM) known as pure GGM [11,12]. The results of this analysis are summarized in Fig. 2. We will also comment on constraints for ordinary gauge mediation in Section 2.2.

Going beyond gauge mediation, we use the LHC data to test the viability of the Snowmass sps [13], the ATLAS SU [14] and the CMS LM [15] benchmark points, which represent a large variety of mediation scenarios (cf. Tab. 1). For comparison we combine and interpret constraints on the CMSSM, pure GGM and the benchmark points in a model independent way in terms of physical squark and gluino masses, in Figs. 5-7.

2 Gauge Mediation

Theories with gauge mediated supersymmetry breaking provide a particularly simple and compelling set-up for addressing theory and phenomenology beyond the Standard Model, see [16] for a review. On the theoretical side, gauge mediation provides an advantage compared to other SUSY-breaking mechanisms (such as gravity mediation) due to its automatic avoidance of unsuppressed flavour changing interactions². Over the last few years there has been a surge of interest in gauge mediation which has led to a significant extension and generalisation of its original realisation. The GGM framework, first

¹In this paper we consider gauge mediation models where the next-to-lightest supersymmetric particles (NLSP) are stable on collider timescales. Limits on models where the NLSP decays promptly into photons and gravitinos are presented in [4].

²On the other hand, gauge mediation does not provide any straightforward WIMP dark matter candidates. Contrary to gravity mediation, the lightest neutralino in gauge mediation will always ultimately decay to the gravitino, which is the LSP. This rules out neutralino candidates for dark matter in gauge mediation, though not the possibility of gravitino dark matter.

introduced in [17], is suitable for unifying quite general models of gauge mediation in a model-independent way. It requires that supersymmetry breaking is communicated to the Standard Model (MSSM) sector through gauge interactions at the messenger scale.

2.1 Pure general gauge mediation

The GGM formulation (or more precisely pure GGM) is based on the requirement that SUSY-breaking effects in the MSSM should disappear in the limit of vanishing Standard Model gauge couplings. The resulting description does not require precise knowledge of any specific underlying models, which can be weakly or strongly coupled, with explicit messenger sectors or direct mediation, or any combination of the above.

A detailed study of the phenomenology of pure GGM models and their parameter spaces was presented recently in [11, 12]. As alluded to above, in pure GGM we have no direct couplings of the SUSY-breaking sector to the Higgs sector, and therefore the soft parameter B_{μ} is approximately zero at the messenger scale. From this starting point at the high scale M_{mess} a small but viable value of B_{μ} is generated radiatively at the electroweak scale [18,19]. Electroweak symmetry breaking then determines the values of $\tan \beta$ and μ . Since B_{μ} is small, $\tan \beta$ is generally large (between 20 and 70).

The main free parameters of pure GGM models are the gaugino and scalar masses as well as the messenger scale [20,21]. In models with messenger fields transforming in complete and unsplit GUT multiplets, there is a single effective scale Λ_G for the gaugino masses and a single scale Λ_S for the scalars [21]³. Generating Λ_G requires both R-symmetry and supersymmetry breaking while Λ_S is affected only by supersymmetry breaking. For this reason Λ_G and Λ_S are two a priori distinct scales in GGM. In the simplest scenario, ordinary gauge mediation (on which we will comment in the next subsection), one can nevertheless identify these two scales, $\Lambda_G \simeq \Lambda_S$.

In GGM the soft supersymmetry breaking gaugino masses at the messenger scale $M_{\rm mess}$ are given by

$$M_{\tilde{\lambda}_i}(M_{\text{mess}}) = k_i \frac{\alpha_i(M_{\text{mess}})}{4\pi} \Lambda_G$$
 (2.1)

where $k_i = (5/3, 1, 1)$, $k_i \alpha_i$ (no sum) are equal at the GUT scale and α_i are the gauge coupling constants. Similarly, the scalar mass squareds are

$$m_{\tilde{f}}^2(M_{\text{mess}}) = 2 \sum_{i=1}^3 C_i k_i \frac{\alpha_i^2(M_{\text{mess}})}{(4\pi)^2} \Lambda_S^2$$
 (2.2)

where the C_i are the quadratic Casimir operators of the gauge groups.

³More generally, if one does not require unification, there are six distinct Λ scales in GGM: $\Lambda_{G,r}$, $\Lambda_{S,r}$ with r=1,2,3 in GGM [17].

In summary, the value of the high scale $M_{\rm mess}$, together with Λ_G and Λ_S appearing in Eqs. (2.1)-(2.2) at $M_{\rm mess}$ characterise a point in the pure GGM parameter space. In this sense pure GGM is the gauge mediation analogue of the CMSSM and mSUGRA models with Λ_G and Λ_S playing a role similar to the parameters $m_{\frac{1}{2}}$ and m_0 in those models. However these gravity mediated simple realisations are physically quite distinct from the gauge mediated pure GGM framework we analyse here. The main differences in gauge mediation include:

- the gravitino is always the LSP and the NLSP can be long lived and is not necessarily neutral;
- at the high scale the sfermion masses are not identical, in particular the left- and right-handed sfermions have different masses as can be seen from Eq. (2.2);
- M_{mess} is a parameter of the model which is typically much lower than the GUT scale.

Outside the confines of ordinary gauge mediation, where the $\Lambda_G \simeq \Lambda_S$, the pure GGM parameter space is populated by many models that predict different values of the ratio of gaugino to scalar masses, Λ_G/Λ_S . This parameter space was investigated in Refs. [11,12] from which we adopt Figure 1. This figure shows the allowed parameter space of pure GGM in the (Λ_G, Λ_S) plane (before the new LHC constraints are imposed) for a fixed value of $M_{\rm mess} = 10^{10}$ GeV. We used a modified version of SoftSUSY [22], which takes $B_\mu = 0$ as an input and predicts $\tan \beta$ using the electroweak symmetry breaking conditions. Direct experimental searches from the Tevatron and LEP (see [12] for more detail) exclude the black region in Fig. 1 on the left of the Nessie-shaped pure GGM parameter space, not surprisingly it effectively cuts off the lower values of gaugino and scalar masses. Other boundaries of the parameter space arise from requiring that there are no tachyons and no Landau poles, and that SoftSUSY has not encountered convergence problems during the RG evolution between the high and the low scales.

In gauge mediation models with explicit messengers one expects the ratio Λ_G/Λ_S to be close to one (dotted line in Fig. 1), while for direct mediation models the gaugino masses are often suppressed relative to the scalar masses [24–31] (region above the dotted line in Fig. 1). It is also possible to achieve values $\Lambda_G/\Lambda_S > 1$ by increasing the "effective number of messengers" [32–37] (region below the dotted line in Fig. 1).

The discovery potential for pure GGM models during the early stages of the LHC with $\sqrt{s} = 7 \,\text{TeV}$ was addressed in Ref. [12]. The left panels in Fig. 2 show three scans of the parameter space of pure GGM (taken from [12]), at different messenger scales, $M_{\text{mess}} = 10^8 \,\text{GeV}$, $10^{10} \,\text{GeV}$ and $10^{14} \,\text{GeV}$. The regions expected to be most sensitive to pp-scattering at $\sqrt{s} = 7 \,\text{TeV}$, correspond to relatively light gluinos and/or relatively light squarks. In each figure stop mass contours of 500 GeV and 1 TeV are indicated as

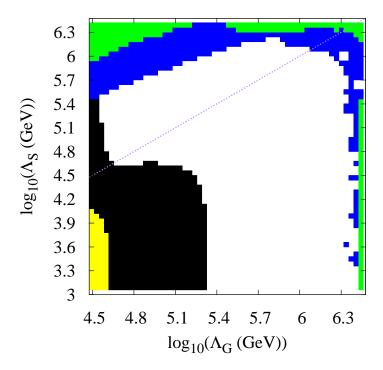


Figure 1: Pure GGM parameter space for intermediate messenger scales, $M_{\rm mess}=10^{10}$ GeV. The dominant constraints excluding various areas around the allowed (white) region are indicated as follows: points in the black region violate the pre-LHC direct search limits, while yellow area is excluded by the presence of tachyons in the spectrum. In the blue region SoftSUSY has not converged and in the green region a coupling reaches a Landau pole during RG evolution. Ordinary gauge mediation lives on the dotted line.

dotted lines, and the 500 GeV and 1 TeV gluino contours are indicated as solid lines⁴. Furthermore, the diagonal dotted red line corresponds to the boundary between neutralino and slepton NLSP. The figures also contain the benchmark points introduced in [12].

We now implement the new experimental constraints on SUSY searches obtained from the ATLAS data on final states with jets, missing energy and no leptons. The details of our analysis of this data are explained in section 3. Our results are obtained from a Monte Carlo simulation of the signal events using Herwig++ [38, 39] and RIVET [40], implementing all the experimental cuts imposed by ATLAS [3]. Combining the four signal regions defined by ATLAS [3] we obtain the constraints shown as the red lines in the right panels of Fig. 2. One can clearly see that already the relatively small data sample of 35 pb⁻¹ provides interesting new bounds on models of pure general gauge mediation.

As one would expect the excluded regions correspond to relatively low gluino and squark masses. This will become clearer in Fig. 6 which shows the GGM exclusion region

⁴In the $M_{\rm mess} = 10^8$ GeV scenario the single dotted contour is for 1 TeV stop masses.

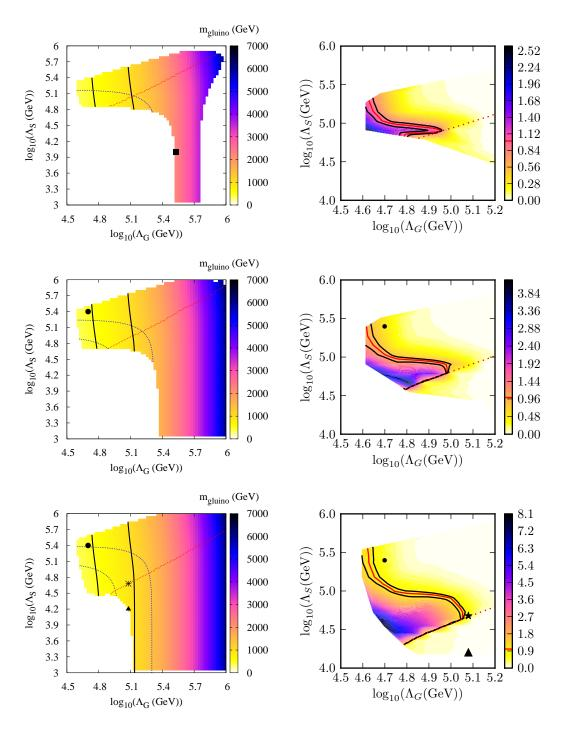


Figure 2: The left panels show the pure GGM parameter space in terms of Λ_G , Λ_S defined in Eqs. (2.1) and (2.2). From top to bottom we have $M_{\rm mess}=10^8\,{\rm GeV}$, $10^{10}\,{\rm GeV}$ and $10^{14}\,{\rm GeV}$. Stop mass contours (500 GeV and 1 TeV) are indicated as dotted lines, and the 500 GeV and 1 TeV gluino lines are solid. The NLSP is neutralino above the diagonal red line and stau below. The panels on the right show 95% exclusion contours derived from the ATLAS search as red lines, and the black lines indicate uncertainties due to scale variations in the NLO cross-section. The colour scale for the right panels shows the expected number of signal events normalised to the exclusion limit. The benchmark points discussed in [23] are shown as a dot (PGM1a middle panel, PGM1b bottom panel), triangle for PGM2, a star for PGM3 and finally a square for PGM4.

directly in terms of the squark and gluino masses (rather than Λ_S and Λ_G). It is interesting to note that there nevertheless exists an allowed narrow wedge shaped region at low values of Λ_S , i.e. for relatively low squarks masses. In this region the NLSP is a stau rather than a neutralino. When the NLSP is the lightest stau, the ATLAS jets plus missing energy search does not constrain the GGM model. As the NLSP is charged the only missing energy in the events comes from the production of neutrinos in the SUSY cascade decays. We would expect that the stau would either be reconstructed as a muon, provided that its time delay reaching the muon chambers is sufficiently short, or the event is rejected due to mismeasurement of the missing transverse energy if its interaction in the muon chambers is not recorded. To be conservative we do not consider these events in this paper. However we emphasize that this is a very interesting region of parameter space as it gives a smoking gun for gauge mediation. This is worthy of further study using a similar approach to that in [41].

We can compare the excluded regions with the previously identified best-fit regions from a global fit to low energy observables performed in [11]. For both $M_{\rm mess}=10^{10}~{\rm GeV}$ and $10^{14}~{\rm GeV}$ the ATLAS search rules out some parameter space which was within the 95% confidence limits of those fits ⁵. For $M_{\rm mess}=10^{10}~{\rm GeV}$ a small region of the previous 68% CL has now been ruled out at low Λ_G and moderate Λ_S . The best-fit points, which lie deep in the stau NLSP region, are unaffected by the ATLAS results. This differs from recent fits of the CMSSM and related models [6], where the best-fit points were more strongly affected, although they still remain within the 95% CL of the pre-LHC fits. The fact that in PGGM the best-fit points lie in the stau NLSP region further motivates a dedicated search for stau NLSPs.

We find that the lowest viable gluino mass which occurs is 380 GeV, a bound which is independent of the messenger scale and the identity of the NLSP. The lowest viable squark mass depends on the messenger and on the NLSP identity. For neutralino NLSP, we find that the lowest allowed squark mass is 735 GeV which happens when the gluino mass is approximately 500 GeV. Since we do not expect the ATLAS search to be sensitive to the stau NLSP region, the lowest permissible squark mass there is reduced to 490 GeV (where the squark mass is defined as the average mass of the first generation squarks). This can be read off from Fig. 6.

2.2 Ordinary gauge mediation

Models of ordinary gauge mediation live on the $\Lambda_G = \Lambda_S$ slice in GGM parameter space. Here, we will also investigate the implications of the ATLAS data on these models.

In contrast to the discussion of the previous section here we will use a more tradi-

⁵For $M_{\text{mess}} = 10^8$ GeV such a fit has not yet been performed.

tional approach where $\tan \beta$ is treated as a free parameter rather than a prediction. This is achieved by deviating from the strict definition of gauge mediation and allowing for appropriate non-gauge couplings between messenger fields and the Higgs sector⁶. This can then generate an input value for B_{μ} at the high/messenger scale which is traded for $\tan \beta$ at the electroweak scale. As a result the essential parameter space is again three-dimensional, Λ , $M_{\rm mess}$ and $\tan \beta$. In this scenario the bound from the new LHC data for long lived NLSPs is fairly insensitive to the messenger mass with $\Lambda < 72\,\text{TeV}$ excluded by the ATLAS results (for $\tan \beta = 10$ although the bounds are relatively independent of this parameter). This limit entirely arises from the event selection C discussed in the next section and corresponds to a squark mass 675 GeV, a gluino mass of 590 GeV and a NLSP (lightest neutralino) mass of 94 GeV.

3 Implementation of the ATLAS event selection and analysis of the data

The ATLAS analysis [3] presents the number of observed events which pass four specific event selection criteria, together with the expected number of Standard Model events. This can be used, together with an estimate of the number of signal events passing the experimental cuts, to determine whether a specific model is ruled out at the 95% confidence level. Alternatively the limits on the cross sections for non-SM processes given in [3] can be used. Here we will do the latter as it already includes most of the statistical analysis.

In order to compare the predictions of a particular BSM model with the ATLAS results we therefore need to calculate the expected number of signal events passing the cuts in each of the four regions (A,B,C,D) defined in Table 1 of Ref. [3]. These regions are designed to target light $\tilde{q}\tilde{q}$, heavy $\tilde{q}\tilde{q}$, $\tilde{g}\tilde{g}$ and $\tilde{g}\tilde{q}$ production respectively, in the CMSSM. This is achieved by imposing different selection criteria on the number of jets (≥ 2 in A and B and ≥ 3 in C and D) as well as on the kinematics (E_T^{miss} , m_{eff} and m_{T2}), see Ref. [3] for details.

Each SUSY model is a point in the MSSM parameter space which is specified by the mass spectrum, SUSY couplings and mixing angles at the electroweak scale. All these are contained in SLHA files produced by SoftSUSY [22] starting from the high-scale input from GGM or any other model.

Given the complexity of the signal processes the calculation of the number of signal events is best achieved using a Monte Carlo event generator, in our case Herwig++ [38,39],

⁶Strictly speaking these extra couplings can also generate new contributions to the Higgs soft masses $m_{H_u}^2$ and $m_{H_d}^2$ but we will ignore these for simplicity.

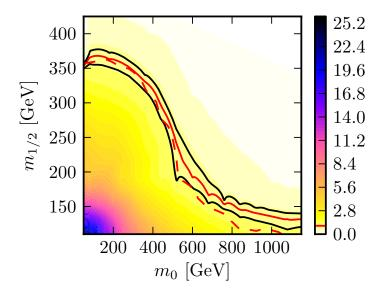


Figure 3: 95% confidence level exclusion limit in the $(m_0, m_{\frac{1}{2}})$ plane for $\tan \beta = 3$, $A_0 = 0$ and $\mu > 0$ in the CMSSM. The solid red line is the result using our signal simulations (the solid black lines show the effect of varying the factorization and renormalisation scales used to calculate the next-to-leading order SUSY production cross sections by a factor of $\frac{1}{2}$ and 2), whereas the dashed red line is the limit obtained by ATLAS in [3]. The colour scale shows the expected number of signal events normalised to the exclusion limit.

to simulate the signal processes for a given SUSY model. The experimental event selection can be implemented using the RIVET [40] analysis framework⁷ to analyse the hadronic final state generated by the Monte Carlo simulation, without the need for a simulation of the detector response.

In principle this is sufficient to calculate the number of expected signal events for any new physics model. However, for most new physics signals the matrix elements implemented in general purpose Monte Carlo event generators are only accurate to leading order in perturbative QCD. Herwig++ was therefore used to simulate three sets of supersymmetric particle production processes for each point in supersymmetric parameter space: a) squark and gluino production, b) the production of an electroweak gaugino in association with a squark or gluino and c) the production of slepton and electroweak gaugino pairs. The fraction of events passing the experimental cuts was then used together with the next-to-leading order cross section calculated using Prospino [43–46] to obtain the number of signal events passing the cuts for each of the four signal regions.

In order to check that our simulations and implementation of the experimental cuts was reliable we checked that we obtained good agreement with the numbers of events

⁷In addition we used the library based on the results of [42] to calculate the m_{T2} variable.

passing the cuts for the CMSSM supersymmetric parameter points in $(m_0, m_{\frac{1}{2}})$ plane for $\tan \beta = 3$, $A_0 = 0$ and $\mu > 0$ supplied as supporting material [47] with [3]. The limit we obtain for the CMSSM using our simulations is in good agreement with that obtained by ATLAS⁸, as can be seen in Fig. 3. These results use the NLO cross sections. As a cross check we have also computed the bounds using the leading-order cross sections. The resulting limits are somewhat lower but show worse agreement with the ATLAS values.

The number of events and the 95% confidence level exclusion limit for pure GGM with $M_{\rm mess}=10^{14}$ GeV is shown in Fig. 4 for each of the four ATLAS-defined regions. This exclusion limit is obtained from the maximum non-SM cross sections of 1.3, 0.35, 1.1 and 0.11 pb, for regions A,B,C and D, respectively given in [3]. As can be seen from Fig. 4 the strongest limit is given by the C and D event selections with D giving the strongest limit at low Λ_S and C the strongest limit for high values of Λ_S . This is consistent with expectations from the design purpose of these regions, since at high Λ_S the squark masses are high and the SUSY cross-section is dominated by $\tilde{g}\tilde{g}$ production, corresponding to ATLAS' region C At lower values of Λ_S we are closer to squark-gluino mass degeneracy and so $\tilde{q}\tilde{g}$ production dominates, and region D provides the best search limits. The combination of parameter space excluded by the various regions is given in the right panels of Fig. 2 for a range of messenger scales.

4 Beyond gauge mediation: Analysis of full set of benchmark points

A number of benchmark points have been proposed for the study of supersymmetric models at high energy colliders. There is a range of motivations for the selection of these points including: satisfying the current experimental constraints, providing the correct relic neutralino abundence to satisfy cosmological limits and comparing the potentials of different experiments. A number of these points, including the most studied sps1a, were designed to study the potential of measuring supersymmetric masses at the LHC and therefore have relatively light mass spectra. As the LHC data now rule out regions of the previously allowed parameter space, nearly half of these points are now excluded. In Table 1 we show effects of the ATLAS 0 leptons SUSY search on the Snowmass sps points, the ATLAS SU points, the CMS LM points and the PGM benchmarks. The columns of the table show the mediation scenario, the calculated cross-sections for each of the regions A,B,C and D, and finally whether the point is ruled out by the data and by which regions. Six of the ten sps points are ruled out by the ATLAS search, including sps1a. Also, four of the SU benchmarks are now excluded, and eight of the sixteen LM benchmarks. The PGM benchmarks proposed in [12] remain allowed by the recent data. Since the proposed

⁸Except in the high m_0 region where there is a significant scale uncertainty for the signal cross section, which we have not included.

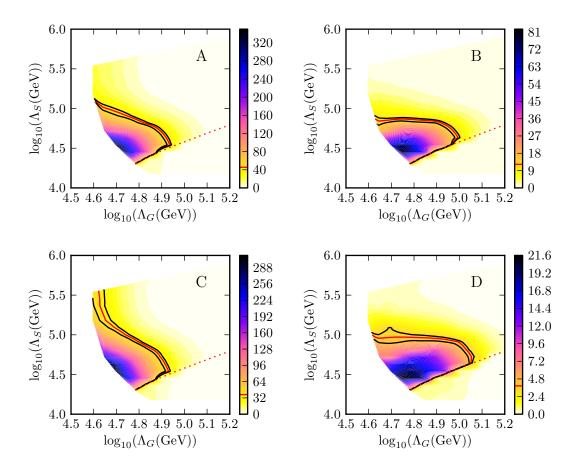


Figure 4: Event rates of pure GGM ($M_{\rm mess}=10^{14}~{\rm GeV}$) in the four signal regions corresponding to different sets of experimental cuts [3]. The shading gives the number of events predicted in our model, after all cuts have been applied. The red line shows the exclusion contour. Below and to the right of the red dotted line the stau is the NLSP whereas above and to the left the NLSP is the lightest neutralino.

benchmarks are mostly at low masses, all the excluded points are ruled out at least by region D, if not by more regions.

| Benchmark point | mediation scenario | σ/pb | | | | status |
|-----------------|---|----------------------|--------|--------|--------|------------------------|
| | | A | В | С | D | ${ m ATLAS~35pb^{-1}}$ |
| ATLAS Limits | | 1.3 | 0.35 | 1.1 | 0.11 | |
| sps1a [13] | CMSSM | 2.031 | 0.933 | 1.731 | 0.418 | A,B,C,D |
| sps1b [13] | CMSSM | 0.120 | 0.089 | 0.098 | 0.067 | allowed |
| sps2 [13] | CMSSM | 0.674 | 0.388 | 0.584 | 0.243 | B,D |
| sps3 [13] | CMSSM | 0.123 | 0.093 | 0.097 | 0.067 | allowed |
| sps4 [13] | CMSSM | 0.334 | 0.199 | 0.309 | 0.144 | D |
| sps5 [13] | CMSSM | 0.606 | 0.328 | 0.541 | 0.190 | D |
| sps6 [13] | CMSSM (non-universal $m_{\frac{1}{2}}$) | 0.721 | 0.416 | 0.584 | 0.226 | B,D |
| sps7 [13] | GMSB ($\tilde{\tau}_1$ NLSP) | 0.022 | 0.016 | 0.023 | 0.015 | allowed |
| sps8 [13] | GMSB $(\tilde{\chi}_1^0 \text{ NLSP})$ | 0.021 | 0.011 | 0.022 | 0.009 | allowed |
| sps9 [13] | AMSB | 0.019* | 0.004* | 0.006* | 0.002* | A,B,C,D |
| SU1 [14] | CMSSM | 0.311 | 0.212 | 0.246 | 0.143 | D |
| SU2 [14] | CMSSM | 0.009 | 0.002 | 0.010 | 0.001 | allowed |
| SU3 [14] | CMSSM | 0.787 | 0.440 | 0.637 | 0.258 | B,D |
| SU4 [14] | CMSSM | 6.723 | 1.174 | 7.064 | 0.406 | A,B,C,D |
| SU6 [14] | CMSSM | 0.140 | 0.101 | 0.115 | 0.074 | allowed |
| SU8a [14] | CMSSM | 0.251 | 0.174 | 0.197 | 0.120 | D |
| SU9 [14] | CMSSM | 0.060 | 0.046 | 0.053 | 0.040 | allowed |
| LM0 [15] | CMSSM | 6.723 | 1.174 | 7.064 | 0.406 | A,B,C,D |
| LM1 [15] | CMSSM | 2.307 | 1.108 | 1.808 | 0.458 | A,B,C,D |
| LM2a [15] | CMSSM | 0.303 | 0.201 | 0.241 | 0.139 | D |
| LM2b [15] | CMSSM | 0.260 | 0.180 | 0.205 | 0.123 | D |
| LM3 [15] | CMSSM | 1.155 | 0.504 | 1.113 | 0.270 | B,C,D |
| LM4 [15] | CMSSM | 0.783 | 0.432 | 0.699 | 0.260 | B,D |
| LM5 [15] | CMSSM | 0.202 | 0.138 | 0.179 | 0.109 | allowed |
| LM6 [15] | CMSSM | 0.127 | 0.094 | 0.099 | 0.068 | allowed |
| LM7 [15] | CMSSM | 0.062 | 0.013 | 0.072 | 0.006 | allowed |
| LM8 [15] | CMSSM | 0.189 | 0.099 | 0.194 | 0.082 | allowed |
| LM9a [15] | CMSSM | 0.238 | 0.029 | 0.358 | 0.015 | allowed |
| LM9b [15] | CMSSM | 0.075 | 0.017 | 0.088 | 0.009 | allowed |
| LM10 [15] | CMSSM | 0.003 | 0.000 | 0.003 | 0.000 | allowed |
| LM11 [15] | CMSSM | 0.358 | 0.223 | 0.311 | 0.166 | D |
| LM12 [15] | CMSSM | 0.037 | 0.008 | 0.043 | 0.004 | allowed |
| LM13 [15] | CMSSM | 2.523 | 0.904 | 2.289 | 0.331 | A,B,C,D |
| PGM1a [12] | pure GGM ($\tilde{\chi}_1^0$ NLSP) | 0.351 | 0.030 | 0.570 | 0.009 | allowed |
| PGM1b [12] | pure GGM ($\tilde{\chi}_1^0$ NLSP) | 0.373 | 0.032 | 0.625 | 0.014 | allowed |
| PGM2 [12] | pure GGM ($\tilde{\tau}_1$ NLSP) | 0.008* | 0.005* | 0.009* | 0.003* | allowed |
| PGM3 [12] | pure GGM $(\tilde{\tau}_1, \tilde{\chi}_1^0 \text{ co-NLSP})$ | 0.140 | 0.103 | 0.121 | 0.086 | allowed |
| PGM4 [12] | pure GGM ($\tilde{\tau}_1$ NLSP) | 0.000 | 0.000 | 0.000 | 0.000 | allowed |

Table 1: Status of SUSY benchmark points. For each point the columns labelled A,B,C and D give the cross section for each of the signal regions used in the ATLAS analysis [3]. The last column shows which of the four regions the point is excluded by using the new data. In the GMSB scenerio the NLSP was taken to be stable on collider time scales. The starred cross sections are computed at leading-order values whereas all the other values are NLO.

5 Conclusions

In this paper we have obtained the first constraints on gauge mediation models of SUSY breaking with long-lived NLSP from 35pb⁻¹ of LHC data at 7 TeV involving jets and missing energy in the final states. In carrying this out we performed an independent Monte Carlo simulation of signal events implementing all experimental constraints imposed by ATLAS in [3].

Our main results are summarized in Fig. 2 and 6 for gauge mediation and in Tab. 1 and Figs. 5 and 7 for a standard set of benchmark points including also non-gauge-mediated models and the CMSSM.

In addition to an interpretation of their results in terms of the CMSSM in [3] ATLAS also presented their results as a limit on a squark and gluino masses in a simplified model which only contained squarks, gluinos and a massless neutralino. The latter tends to increase the search reach by increasing the energy of the visible decay products.

In Figs. 5-7 we interpret and combine the ATLAS constraints on different SUSY models by displaying them in terms of physical squark and gluino masses. Fig. 5 shows the mapping of the CMSSM m_0 - $m_{1/2}$ parameter space into the squark-gluino mass space. We note that the region $m_{\tilde{g}} \lesssim m_{\tilde{q}}$ is not accessible in any of the models we have studied due to the effects of the gluino masses on the squark masses during the RG evolution⁹. In general, constraints in the squark and gluino plane are similar in all the models we have considered (see Figs. 5-7), despite significant differences in the mass spectra of the other sparticles. Importantly however this can change if the (N)LSP is not the lightest neutralino as can be seen in Fig. 6. Moreover this limit is always weaker than that obtained in the simplified model due to the non-vanishing neutralino mass.

⁹While close to one in the CMSSM, the slope of the boundary in $(m_{\tilde{q}}, m_{\tilde{q}})$ is model dependent.

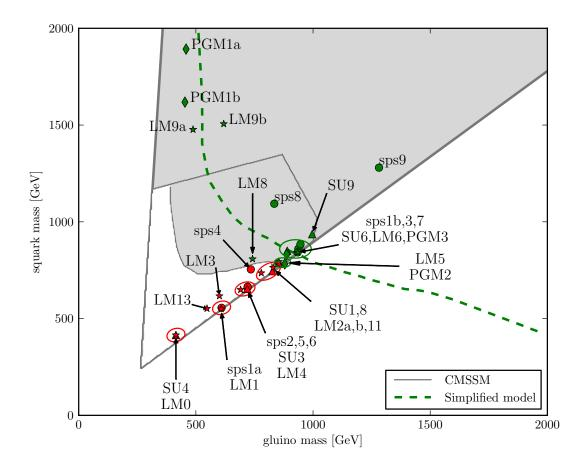


Figure 5: This plot shows constraints on the CMSSM for $\tan \beta = 3$, $A_0 = 0$ and $\mu > 0$ mapped into the plane of the physical squark (average of first generation) and gluino masses. The kite-shaped area shows the same region of parameter space as in Fig. 3. The grey area is still allowed, whereas the white region inside the kite is now excluded by the ATLAS measurements [3]. The region below the diagonal $m_{\tilde{g}} \lesssim m_{\tilde{q}}$ is not part of the CMSSM parameter space due to the influence of the gluino mass on the squark masses during the RG evolution. The dashed green line gives the constraints obtained from a simplified model (containing only squarks and gluinos and a massless neutralino) in [3]. The reduced sensitivity in the CMSSM is mainly due to the non-negligible neutralino mass. The labelled points are the benchmark points of Tab. 1. Red points are now excluded whereas green points are still viable.

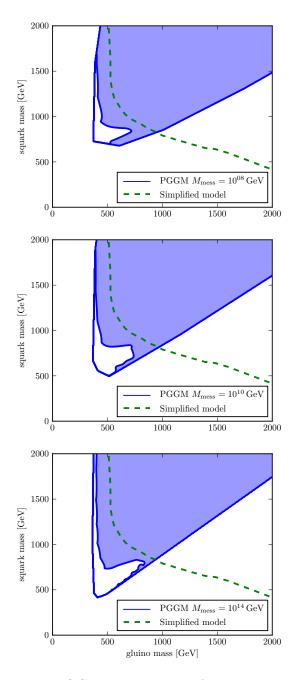


Figure 6: Constraints on pure GGM in the plane of the physical squark and gluino masses for three different choices of the messenger scale. For each plot the wedge-shaped region shows the previously allowed parameter space, the white part of which is now excluded by the ATLAS results. As before, the green dashed line gives the constraints for a simplified model. The allowed region near the lower boundary of the model space is due to lack of missing energy in models with a stau NLSP.

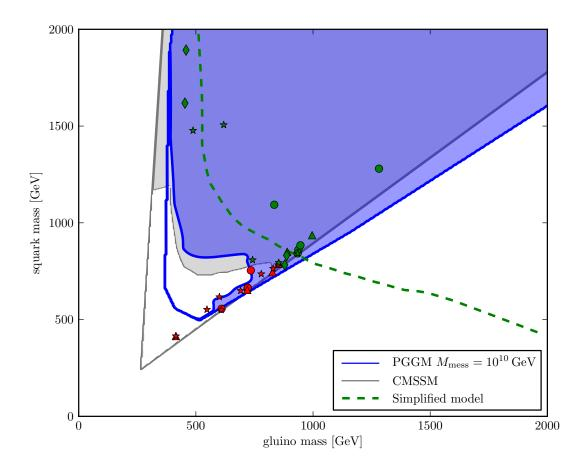


Figure 7: Compilation of constraints in terms of physical gluino and squark masses in different models of SUSY breaking. In blue we show constraints in a pure GGM model with $M_{\rm mess}=10^{10}$ GeV. The white region enclosed in blue lines is now excluded by the LHC data [3], the shaded area is still viable. For comparsion we show in grey the allowed and excluded regions for the CMSSM (with $\tan\beta=3$, $A_0=0$ and $\mu>0$). We also show benchmark points from [12–15] (see Tab. 1). The green points are still allowed, and the red ones are now excluded. The dashed green line gives the constraints obtained from a simplified model as before.

Acknowledgements

We are grateful to Steve Abel, Alan Barr, Oliver Buchmueller, T. J. Khoo and Chris Lester for interesting discussions and comments. This work was supported by STFC.

References

- [1] **CMS** Collaboration, V. Khachatryan et. al., Search for Supersymmetry in pp Collisions at 7 TeV in Events with Jets and Missing Transverse Energy, 1101.1628.
- [2] **ATLAS** Collaboration, J. B. G. da Costa et. al., Search for supersymmetry using final states with one lepton, jets, and missing transverse momentum with the ATLAS detector in sqrts = 7 TeV pp, 1102.2357.
- [3] ATLAS Collaboration, J. B. G. da Costa et. al., Search for squarks and gluinos using final states with jets and missing transverse momentum with the ATLAS detector in sqrt(s) = 7 TeV proton-proton collisions, 1102.5290.
- [4] **CMS** Collaboration, S. Chatrchyan et. al., Search for Supersymmetry in pp Collisions at sqrt(s) = 7 TeV in Events with Two Photons and Missing Transverse Energy, 1103.0953.
- [5] B. C. Allanach, Impact of CMS Multi-jets and Missing Energy Search on CMSSM Fits, 1102.3149.
- [6] O. Buchmueller et. al., Implications of Initial LHC Searches for Supersymmetry, 1102.4585.
- [7] P. Bechtle et al., What if the LHC does not find supersymmetry in the sqrt(s)=7 TeV run?," 1102.4693.
- [8] B. C. Allanach, T. J. Khoo, C. G. Lester and S. L. Williams, *The impact of the ATLAS zero-lepton, jets and missing momentum search on a CMSSM fit*, 1103.0969.
- [9] S. Akula, N. Chen, D. Feldman, M. Liu, Z. Liu, P. Nath and G. Peim, *Interpreting the First CMS and ATLAS SUSY Results*, 1103.1197.
- [10] S. Akula, D. Feldman, Z. Liu, P. Nath and G. Peim, New Constraints on Dark Matter from CMS and ATLAS Data, 1103.5061.
- [11] S. Abel, M. J. Dolan, J. Jaeckel and V. V. Khoze, *Phenomenology of Pure General Gauge Mediation*, *JHEP* **12** (2009) 001 [0910.2674].

- [12] S. Abel, M. J. Dolan, J. Jaeckel and V. V. Khoze, Pure General Gauge Mediation for Early LHC Searches, JHEP 12 (2010) 049 [1009.1164].
- [13] B. C. Allanach et. al., The Snowmass points and slopes: Benchmarks for SUSY searches, Eur. Phys. J. C25 (2002) 113–123 [hep-ph/0202233].
- [14] **The ATLAS** Collaboration, G. Aad et. al., Expected Performance of the ATLAS Experiment Detector, Trigger and Physics, 0901.0512.
- [15] **CMS** Collaboration, G. L. Bayatian et. al., CMS technical design report, volume II: Physics performance, J. Phys. **G34** (2007) 995–1579.
- [16] G. F. Giudice and R. Rattazzi, *Theories with gauge-mediated supersymmetry breaking*, *Phys. Rept.* **322** (1999) 419–499 [hep-ph/9801271].
- [17] P. Meade, N. Seiberg and D. Shih, *General Gauge Mediation*, *Prog. Theor. Phys. Suppl.* **177** (2009) 143–158 [0801.3278].
- [18] R. Rattazzi and U. Sarid, Large tan Beta in gauge mediated SUSY breaking models, Nucl. Phys. B501 (1997) 297–331 [hep-ph/9612464].
- [19] K. Babu, C. F. Kolda and F. Wilczek, Experimental consequences of a minimal messenger model for supersymmetry breaking, Phys.Rev.Lett. 77 (1996) 3070–3073 [hep-ph/9605408].
- [20] J. Jaeckel, V. V. Khoze and C. Wymant, Mass Sum Rules and the Role of the Messenger Scale in General Gauge Mediation, 1102.1589.
- [21] J. Jaeckel, V. V. Khoze and C. Wymant, RG Invariants, Unification and the Role of the Messenger Scale in General Gauge Mediation, 1103.1843.
- [22] B. C. Allanach, SOFTSUSY: a program for calculating supersymmetric spectra, Comput. Phys. Commun. 143 (2002) 305–331 [hep-ph/0104145].
- [23] S. Abel, M. J. Dolan, J. Jaeckel and V. V. Khoze, Pure General Gauge Mediation for Early LHC Searches, 1009.1164.
- [24] K. I. Izawa, Y. Nomura, K. Tobe and T. Yanagida, Direct-transmission models of dynamical supersymmetry breaking, Phys. Rev. D56 (1997) 2886–2892 [hep-ph/9705228].
- [25] R. Kitano, H. Ooguri and Y. Ookouchi, Direct mediation of meta-stable supersymmetry breaking, Phys. Rev. D75 (2007) 045022 [hep-ph/0612139].
- [26] C. Csaki, Y. Shirman and J. Terning, A simple model of low-scale direct gauge mediation, JHEP 05 (2007) 099 [hep-ph/0612241].

- [27] S. Abel, C. Durnford, J. Jaeckel and V. V. Khoze, Dynamical breaking of $U(1)_R$ and supersymmetry in a metastable vacuum, Phys. Lett. **B661** (2008) 201–209 [0707.2958].
- [28] S. A. Abel, C. Durnford, J. Jaeckel and V. V. Khoze, *Patterns of Gauge Mediation in Metastable SUSY Breaking*, *JHEP* **02** (2008) 074 [0712.1812].
- [29] S. Abel, J. Jaeckel, V. V. Khoze and L. Matos, On the Diversity of Gauge Mediation: Footprints of Dynamical SUSY Breaking, JHEP 03 (2009) 017 [0812.3119].
- [30] Z. Komargodski and D. Shih, Notes on SUSY and R-Symmetry Breaking in Wess-Zumino Models, JHEP **04** (2009) 093 [0902.0030].
- [31] S. A. Abel, J. Jaeckel and V. V. Khoze, Gaugino versus Sfermion Masses in Gauge Mediation, Phys. Lett. **B682** (2010) 441–445 [0907.0658].
- [32] D. E. Kaplan, G. D. Kribs and M. Schmaltz, Supersymmetry breaking through transparent extra dimensions, Phys. Rev. **D62** (2000) 035010 [hep-ph/9911293].
- [33] Z. Chacko, M. A. Luty, A. E. Nelson and E. Ponton, *Gaugino mediated supersymmetry breaking*, *JHEP* **01** (2000) 003 [hep-ph/9911323].
- [34] C. Csaki, J. Erlich, C. Grojean and G. D. Kribs, 4D constructions of supersymmetric extra dimensions and gaugino mediation, Phys. Rev. **D65** (2002) 015003 [hep-ph/0106044].
- [35] C. Cheung, A. L. Fitzpatrick and D. Shih, (Extra)Ordinary Gauge Mediation, JHEP 07 (2008) 054 [0710.3585].
- [36] M. McGarrie, General Gauge Mediation and Deconstruction, JHEP 11 (2010) 152 [1009.0012].
- [37] D. Green, A. Katz and Z. Komargodski, *Direct Gaugino Mediation*, *Phys. Rev. Lett.* **106** (2011) 061801 [1008.2215].
- [38] M. Bahr et. al., Herwig++ Physics and Manual, Eur. Phys. J. C58 (2008) 639–707 [0803.0883].
- [39] S. Gieseke et. al., Herwig++ 2.5 Release Note, 1102.1672.
- [40] A. Buckley et. al., Rivet user manual, 1003.0694.
- [41] **ATLAS** Collaboration, G. Aad et. al., Search for stable hadronising squarks and gluinos with the ATLAS experiment at the LHC, 1103.1984.
- [42] H.-C. Cheng and Z. Han, Minimal Kinematic Constraints and MT2, JHEP 12 (2008) 063 [0810.5178].

- [43] W. Beenakker, R. Hopker, M. Spira and P. M. Zerwas, Squark and gluino production at hadron colliders, Nucl. Phys. **B492** (1997) 51–103 [hep-ph/9610490].
- [44] W. Beenakker et. al., The Production of charginos / neutralinos and sleptons at hadron colliders, Phys. Rev. Lett. 83 (1999) 3780–3783 [hep-ph/9906298].
- [45] M. Spira, Higgs and SUSY particle production at hadron colliders, hep-ph/0211145.
- [46] T. Plehn, Measuring the MSSM Lagrangean, Czech. J. Phys. **55** (2005) B213–B220 [hep-ph/0410063].
- [47] **The ATLAS** Collaboration, J. B. G. da Costa *et. al.*, http://atlas.web.cern.ch/Atlas/GROUPS/PHYSICS/PAPERS/susy-0lepton_01, .